Lab on a Chip

PAPER

View Article Online
View Journal | View Issue

Cite this: *Lab Chip*, 2026, **26**, 2330

3D ECM-inflammation model on a microfluidic chip for neutrophil transmigration from whole blood investigations

Shide Bakhtiari, * Vanessa Velasco and Ronald W. Davis

Neutrophils have been linked to several inflammation diseases. To study the role of neutrophils in inflammation diseases and conditions, *in vitro* inflammation assays have been developed. Two drawbacks of these assays include the reliance on pre-processing techniques to isolate neutrophils and 2D migration analysis. These assays limit the physiological relevance of *in vivo* neutrophil migration which involves other blood components and the transmigration of 3D extracellular matrix-tissue environments. Extracellular matrices regulate neutrophil activation and deformation – important factors in the study of neutrophil migration behavior. To address these limitations, we have successfully created a microfluidic chip that recreates an inflammation event and directly isolates neutrophils from a small volume of whole blood using a 3D extracellular matrix. We optimized our platform by adjusting the extracellular matrix collagen, chemoattractant, and blood concentrations to maximize neutrophil yield. Six individual blood samples showed a range of 30–70 isolated neutrophils per mm^2 from whole blood with 100% viability and purity using 2 mg mL^{-1} extracellular matrix collagen and 150 nM fMLP concentrations. Using this preliminary data, we performed a regression analysis to examine the effect of blood component quantities – white blood cells, red blood cells, neutrophils, and platelets – on the number of isolated neutrophils. The regression analysis revealed that the number of platelets possibly affects the number of transmigrated neutrophils conforming to a non-linear second-degree polynomial function, with an R^2 of 0.88. Our findings highlight the potential of our platform to facilitate and improve the understanding of neutrophil migration and invasion in inflammation resolution, diseases, and treatments.

Received 4th June 2025,
Accepted 5th January 2026

DOI: 10.1039/d5lc00554j

rsc.li/loc

1 Introduction

Neutrophils or polymorphonuclear leukocytes (PMNs) are the most prevalent white blood cells in humans. They form an important part of the innate immune system and are key players during the inflammation process, acting as the first-line responders in the event of infection or inflammation.[1–3] They migrate directionally by responding to chemical gradients produced by chemokines released at the site of inflammation.[4] The chemokines bind to surface receptors on the neutrophils, inducing intracellular signaling cascades that control cytoskeletal rearrangements and migration towards the inflamed or infected tissue as well as activate immune responses.[5,6] Neutrophils contribute in the development of inflammation diseases and conditions, including autoimmune disorders, atherosclerosis, multiple sclerosis, rheumatoid arthritis and sepsis, by participating in acute and chronic immune reactions.[7] In these diseases, unregulated neutrophil transmigration delays resolution of inflammation and leads to tissue damage. This abnormal trafficking sustains chronic inflammation by a continuous or inhibited[8] recruitment of neutrophils that worsens tissue injury.[9,10] To understand the role of neutrophils in inflammation, especially in chronic inflammation diseases and conditions, inflammation models are required.

Current inflammation models including animal-based zebrafish and rats, continue to enrich our understanding of inflammation mechanisms, but the complex environment in an animal does not allow the determination of specific influences on neutrophil behavior, and the relevance of these models to human biology remains uncertain, as approximately 90% of animal studies fail to translate to human clinical outcomes.[11] Therefore, advanced *in vitro* microfluidic systems and techniques have been developed to study neutrophil behavior, chemotaxis, and migration dynamics in inflammation. However, most systems rely on 2D surface migration, limiting the relevance of the 3D extracellular matrix and tissue environments that neutrophils must transverse during inflammation events. Although some studies investigated neutrophil migration behavior in hydrogel-based assays during an inflammation challenge,[12,13]

Stanford Genome Technology Center (SGTC), Stanford University, Palo Alto, CA 94304, USA. E-mail: shide68@stanford.edu

these microfluidic platforms, still, require the use of isolated neutrophils achieved through conventional density gradient centrifugation or magnetic-activated cell sorting.[14] Centrifugation-based techniques are relatively simple but require large blood volumes, and subject cells to mechanical stress, along with osmotic or thermal shock.[15] Since neutrophils are sensitive, this may have adverse effects on the immune phenotype[16,17] and viability.[18,19] Magnetic-based cell separation while less laborious has shown to alter migration of neutrophils.[20] Thus, more recently, microfluidic models have eliminated the need for isolated neutrophils and have implemented the use of whole blood. One platform captured neutrophils directly from whole blood using adhesion molecules (*e.g.*, P-selectin, E-selectin, fibronectin) or antibody-coated surfaces.[21,22] Another system has shown that strategic microfluidic channel design and microfabricated posts restrict red bloods cells but allow neutrophils to migrate from whole blood towards a chemoattractant gradient (for example, fMLP).[23] Although, these setups do replicate some aspects of *in vivo*-like neutrophil migration from blood to inflamed tissues, they lack the 3D extracellular matrix-tissue environment and are mostly useful for neutrophil adhesion, rolling, and crawling studies in the early steps of migration.[24] 3D extracellular matrix (ECM) forms a complex network of proteins that are accountable for cell locomotion support, immune cell interactions, and essential biochemical and mechanical signals that regulate neutrophil activation and deformation. By activating receptors like integrins, the ECM controls adhesion, signaling, and migration dynamics. In contrast, 2D environments are unable to recreate the dynamic and intricate interactions between cells and ECM proteins, leading to a knowledge gap in cell migration. Furthermore, none of the current systems have successfully reproduced a physiologically relevant 3D ECM structure interfaced with whole blood.

In this work, we developed a novel microfluidic platform that can isolate neutrophils from whole blood using a 3D ECM. The device consists of two chambers: one containing whole blood layered on top of an ECM and the bottom chamber containing a pathogen-like agent, simulating inflammation. Neutrophils migrate through the ECM between the two compartments under a chemoattractant gradient. By examining the ECM collagen, chemoattractant, and blood concentrations, we optimized the platform to isolate neutrophils in the bottom chamber without the contamination of other blood cell types or components. Post-transmigrated neutrophils were easily quantified and optically assessed for viability within the bottom chamber. Using our platform, we isolated neutrophils from six different individuals and quantified their migrated neutrophil populations. We observed differences in the number of transmigrated neutrophils between healthy samples (donor). Through regression analysis, we explored the influence of blood components – white blood cells (WBCs), red blood cells (RBCs), neutrophils, and platelets on the number of isolated neutrophils. Our preliminary data indicated that the number of platelets is likely to influence the number of transmigrated neutrophils, following a non-linear saturation model. These results show that our platform, as a more physiologically relevant inflammation model, can be used to enhance the understanding of neutrophil migration in immune responses, while simplifying neutrophil isolation and enabling the real-time monitoring of post-transmigration behavior. This tool has potential applications in examining neutrophil immune response and resolution mechanisms involved in inflammation diseases and treatments.

2 Material and methods

2.1 Microchip design

We fabricated an upper and lower well platform that mimicked the blood–ECM interface that neutrophils transverse during inflammation events (Fig. 1). Whole blood was placed in the upper well array (Fig. 1(A)), while the bottom chambers contained chemoattractant and captured the migrated neutrophils (Fig. 1(C)). A polycarbonate filter underlaid by an ECM module to simulate the extracellular matrix environment, occupied the space between the top and bottom wells (Fig. 1(B)). Channels running across the bottom wells with inlet and outlet ports at the top well allowed for the injection of chemoattractant.

2.2 Microchip fabrication

The microdevices were fabricated from: acrylic sheets of two different thicknesses (3 mm and 1 mm, McMaster), double-sided adhesive (DSA, ARcare8939), 35 mm glass coverslips (MATTEK CORP), and polycarbonate membrane filters (10 or 20 μM pore size, 13 mm diameter, Millipore, Sigma). Using a laser cutter (Trotec, SP 500), the acrylic and DSA layers were cut to form the top blood and bottom chambers as well as the intermediate adhesive layers. The 1 mm acrylic layer served as the bottom chamber (the chamber containing transmigrated neutrophils) and consisted of three wells, 7 mm in diameter. While the 3 mm acrylic layer was used as the top chamber (blood chamber), also possessing three wells, 11 mm diameter. The DSAs were cut into three distinct designs: the first layer helped to form the bottom chambers and channel patterns, the second layer was identical to the 1 mm acrylic design and was used to adhere the 1 mm acrylic and membrane filter, and the third layer matched the 3 mm acrylic design and connected the membrane filter to the 3 mm acrylic.

Before device assembly, all the acrylic components were rinsed with isopropyl alcohol (IPA) and air-dried. Glass coverslips were immersed and sonicated with autoclaved water containing 200 μL of Liquinox detergent for 30 minutes, and then washed successively with DI water, acetone, methanol, and IPA. Glass coverslips were dried with compressed air and visually inspected for cleanliness. To improve DSA adhesion and create a suitable cell environment, the dry coverslips were plasma treated under 0.1 Torr at medium power for 1 minute. Additionally, to

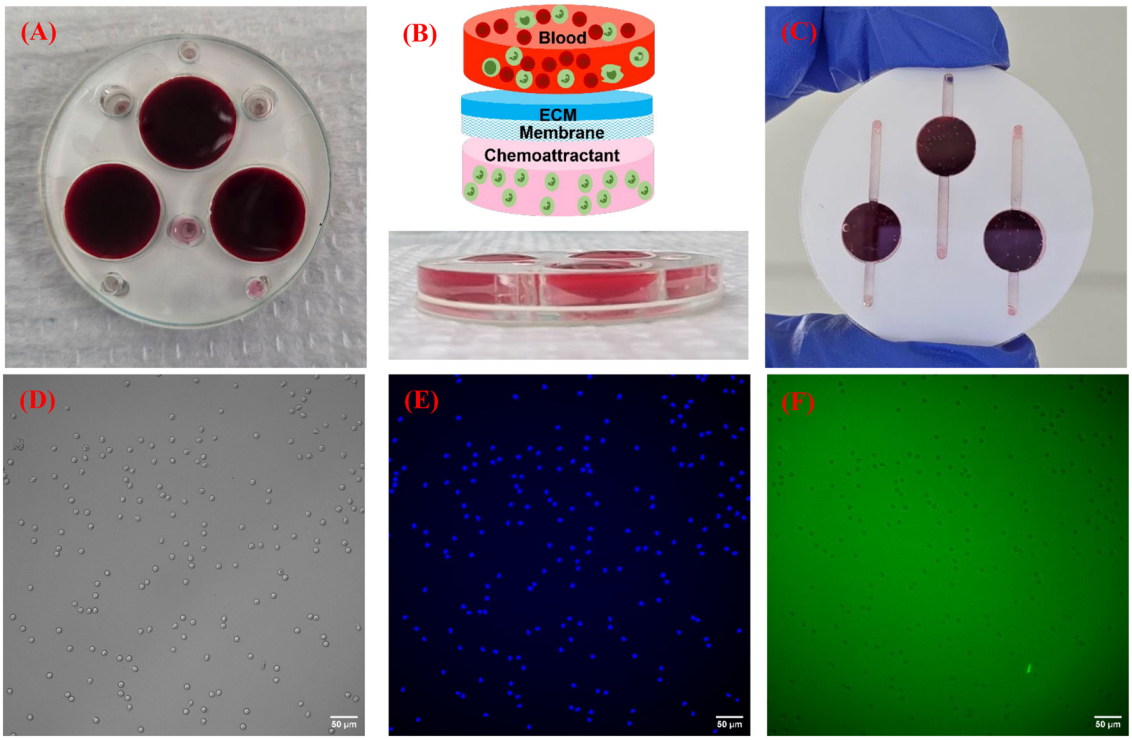

Fig. 1 Images of the microfluidic chip. (A) Top view image showing contained blood sample in the individual wells and the transmigration chamber inlet and outlet ports. (B) Schematic and real side view images showing how the ECM gel layer interfaces the blood sample and bottom (transmigration) chamber. (C) Bottom view image displaying well-defined channels with no blood in the transmigration chambers. Isolated neutrophils in the transmigration chamber after 2 hours are shown, where images were captured with a 20× objective. (D) DIC image. (E) NucBlue-stained image of neutrophils highlighting their nuclei. (F) FITC image showing no presence of dead cells (or positive NucGreen staining).

enhance surface hydrophilicity and ECM adhesion to the 3 mm acrylic top layer, UV ozone treatment was applied for 20 minutes on one side and 10 minutes on the other side before assembly.

The device was assembled by placing the cleaned coverslip on a lint-free paper surface. All layers were carefully aligned at each step to ensure channel port functionality. The first layer of DSA was adhered to the coverslip. The 1 mm acrylic layer was then attached, followed by the second layer of DSA. The polycarbonate membrane filter was gently placed at the center of each bottom well by pressing the edge of the filters onto the exposed adhesive. Next, the third layer of DSA was attached. At the top, the 3 mm acrylic layer was added to form the top chamber. Finally, the assembled device was inspected to ensure proper alignment, adhesion, and component integrity.

2.3 Extracellular matrix preparation

ECM was prepared by combining a rat tail type I collagen (Gibco, Thermo Fisher Scientific) with hydrogel (Geltrex LDEV-Free Reduced Growth Factor Basement Membrane Matrix, Gibco, Thermo Fisher Scientific). The hydrogel, Geltrex, was diluted with Iscove's modified Dulbecco's medium (IMDM) to a concentration of 3 mg mL^{-1}, following the manufacturer's instruction. Collagen stock (3 mg mL^{-1}) was neutralized on ice according to the manufacturer's protocol by mixing with sterile 10× PBS (Gibco, Thermo Fisher Scientific), sterile distilled water (dH_2O, Life Technology), and sterile 1 N NaOH (Sigma Aldrich) to achieve a neutral pH. Collagen solutions at 0.5, 1, and 2 mg mL^{-1} were then prepared by calculating and mixing the appropriate volumes of stock and reagents. All calculations followed the manufacturer's guidelines to ensure accuracy. The ECM was prepared on a bed of crushed ice and in a sterile culture hood to maintain component stability as well as a contamination-free environment. The hydrogel and collagen solutions were combined to form a homogeneous ECM mixture. A volume of 150 μL of the ECM solution was then poured within each top chamber well (11 mm diameter) to cover the polycarbonate filter surface (Fig. 2). Finally, the ECM-coated microdevice was transferred to an incubator maintained at 37 °C for 30 minutes, to polymerize and form a stable gel.

2.4 Neutrophil isolation

Blood samples were collected from the Stanford Blood Center. All blood components and parameters were counted using a Sysmex XN-330 hematology analyzer.

Isolated neutrophils were required for device characterization experiments. For this, an EasySep Human

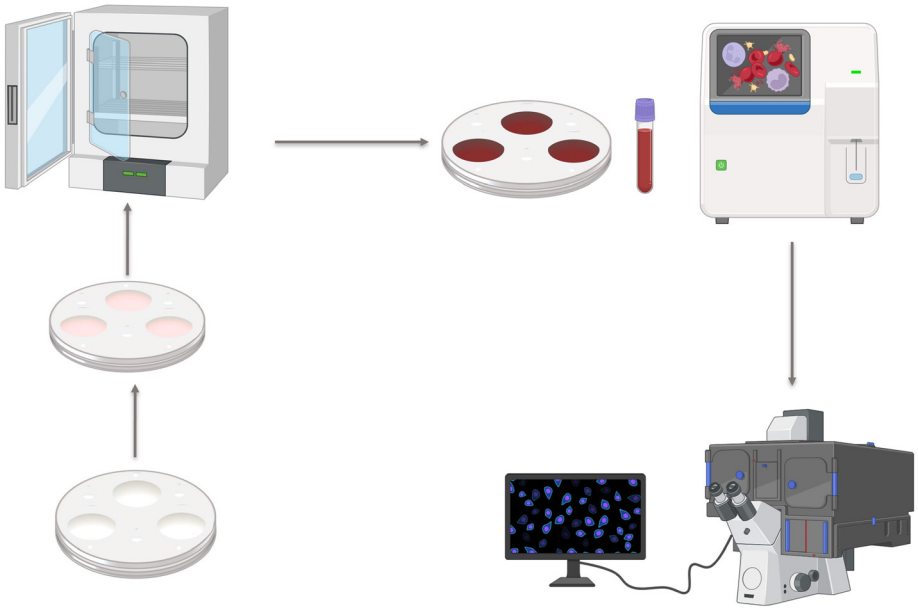

Fig. 2 Schematic of the inflammation model experimental workflow. The microfluidic chip was cleaned and manually fabricated. The ECM was prepared and poured into the microfluidic chip, followed by polymerization in the incubator. The blood sample was stained and introduced into the microfluidic chip. Chemoattractant was injected into the bottom channel to induce an inflammation challenge. Blood components were analyzed using a hematology analyzer. The chip was then incubated in the microscope at 37 °C with 5% CO_2. 2 hours later, stained and transmigrated neutrophils were visualized under the microscope.

Direct Neutrophil Isolation kit (Stemcell) was used following the manufacturer's protocol. Briefly, the blood sample was gently mixed and 1 mL was taken for isolation. 50 μL of the isolation cocktail was added and mixed well, followed by 50 μL of RapidSpheres (vortexed for 30 seconds prior to use). The mixture was gently mixed and incubated at room temperature (RT) for 5 minutes. Next, 3 mL of warm DPBS solution with 1 mM EDTA solution was added and gently mixed. For the second isolation step, the tube was placed inside the EasySep magnet for 10 minutes. The enriched cell suspensions were then pipetted into a new tube. 50 μL of RapidSpheres was added into the tube with the enriched cells. The sample was incubated and mixed at RT for 5 minutes, then again 5 minutes on the EasySep magnet. For the third isolation, the clear fraction was collected into a new tube and placed in the magnet for a final 5 minutes. The enriched cell suspension was carefully transferred into a tube and centrifuged for 10 minutes at 1600 rpm. Afterwards, the supernatant was aspirated, and the cell pellet was resuspended in media. Finally, the cells were counted and adjusted to 2.2×10^6 cells per mL concentration.

2.5 *In vitro* inflammation model workflow

Initially, magnetically isolated neutrophils or neutrophils within whole blood samples were stained with NucBlue (Thermo Fisher Scientific) at 80 μL mL^{-1} to identify neutrophil nuclei as well as with NucGreen at 40 μL mL^{-1} for cell viability assessment. Next, 200 μL of the sample were loaded into the top chambers of the microfluidic device. Subsequently, the chemoattractant fMLP (*N*-formylmethionyl-leucyl-phenylalanine, Sigma) was diluted in RPMI-1640 to achieve final concentrations of 50 nM, 100 nM, 150 nM, 300 nM, or 1 μM; then, 65 μL of the obtained solution was injected into the bottom chambers. The microdevice was placed in a microscope within a humidity-controlled chamber at 37 °C and 5% CO_2 for optimal live-cell imaging conditions. Images of migrated cells at the bottom chamber were recorded, after 2 hours. Schematic of the experimental workflow showing all the steps can be found in Fig. 2.

2.6 Fluorescence microscopy & analysis

NucBlue stained neutrophils were monitored using an Olympus IX-83 inverted live-cell microscope with a motorized *XYZ* stage for accurate positioning of the sample. The central area (~13 mm^2) of the bottom wells where isolated neutrophils accumulated was imaged and stitched together using the CellSens software of the microscope. Differential interference contrast (DIC) and fluorescence channels, DAPI and FITC, were utilized with a 20× objective lens to image migrated neutrophils (Fig. 1D–F). Isolated neutrophils and their viability, in the bottom well within this central area were counted and analyzed using FIJI software. This cell count was divided by the stitched image area (cells per mm^2) and defined as the transmigrated neutrophil population. To confirm that transmigrated cells were neutrophils, we stained nuclei with NucBlue (DAPI) and labeled cells with CD66b–AF647 and, in a subset of experiments, CD16b–AF647, both

neutrophil-specific surface markers in human blood. All experiments were performed using blood from two donors. In the bottom chamber, every transmigrated cell showed a NucBlue-stained nucleus and was labeled with CD66b and, in the backup condition, with CD16b, confirming neutrophil identity. Representative 20× and 40× images (see Fig. S1) illustrate these all transmigrated cells are neutrophils. In 40× images of the bottom chamber (see Fig. S2), all transmigrated cells exhibited the typical multi-lobed nuclei of neutrophils, and no other blood cell types were detected.

3 Results

3.1 Optimization of ECM collagen concentration

Different collagen concentrations can impact the ECM structure, primarily by altering pore size.[25] To determine the optimal pore size of the ECM for neutrophil isolation, we tested the impact of 0.5, 1, and 2 mg mL^{-1} collagen concentrations. To do this, isolated neutrophils were added to the top chamber, while fMLP or chemoattractant was absent at the bottom chamber. We observed that increasing the ECM collagen concentration, decreased the number of neutrophils per mm^2 which transmigrated to the lower chamber (Fig. 3). At 0.5 mg mL^{-1}, an average of 400 neutrophils per mm^2 transmigrated through the matrix. However, increasing the concentration of collagen to 1 mg mL^{-1}, drastically decreased the number of neutrophils per mm^2 to around 100. In the highest concentration tested (2 mg mL^{-1}), almost zero neutrophils were observed at the bottom chamber. These results demonstrate that under our conditions, neutrophil transmigration is minimal without a chemoattractant, confirming the suitability of the ECM configuration for subsequent chemotaxis assays and serving as a negative control.

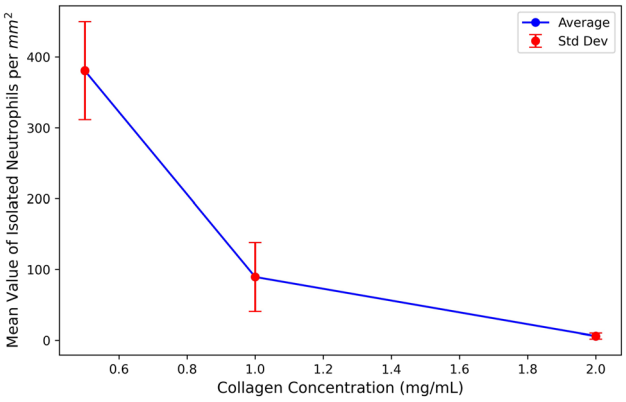

Fig. 3 Effect of collagen concentration on the number of migrated neutrophils through collagen–Geltrex ECM. Human neutrophils were magnetically isolated from whole blood, prepared to 2.2 × 10^6 cells per mL concentration, and allowed to migrate into ECMs with different collagen concentration (0.5, 1 & 2 mg mL^{-1}) to find optimum collagen concentration. Each data point represents the average value from three replicates (n = 3), where the bars show the plus and minus standard deviation. The minimum migration was observed at 2 mg mL^{-1} collagen concentration.

Our studies showed that with higher concentrations of collagen, the pore size of the matrix was likely reduced, thus hindering the movement of neutrophils into the matrix. This experiment was critical in optimizing the structure of collagen and finding the appropriate pore size that was suitable for further studies on neutrophil migration and inflammation. If the matrix pore size was too large, the neutrophils can easily pass to the bottom chamber without inflammation induction. In contrast, higher concentrations of collagen generated denser matrixes with smaller pores sizes that limit neutrophil passage, unless they undergo morphology changes (*i.e.*, spreading) caused by chemoattractant interactions. These reduced pore sizes also ensured that other blood cells or components do not trespass into the bottom chamber.

3.2 Optimization of fMLP concentration

To enhance the number of isolated neutrophils in the bottom chamber while preserving their viability, we tested various fMLP concentrations (50, 100, and 150 nM). For this, magnetically isolated neutrophils were applied to the top of ECMs (2 mg mL^{-1} collagen), fMLP was injected to the bottom chamber, and neutrophils were allowed to migrate into the bottom chamber where cells were counted and viability was assessed with a fluorescent NucGreen dye.

Our data (Fig. 4) indicated that with the increase of fMLP concentration, the number of isolated neutrophils in the bottom chamber was also increased. For 50 nM of fMLP, an average of ~700 neutrophils per mm^2 was observed, while at 100 nM, ~1000 neutrophils per mm^2 were quantified. Finally, ~1500 neutrophils per mm^2 were recorded in the case of 150 nM. In all fMLP conditions, no dead cells were observed within the two hour experimental period. The rise in the number of isolated neutrophils ascertains that 100–150 nM fMLP concentrations provide an adequate chemotactic stimulus without affecting the viability of the cells.

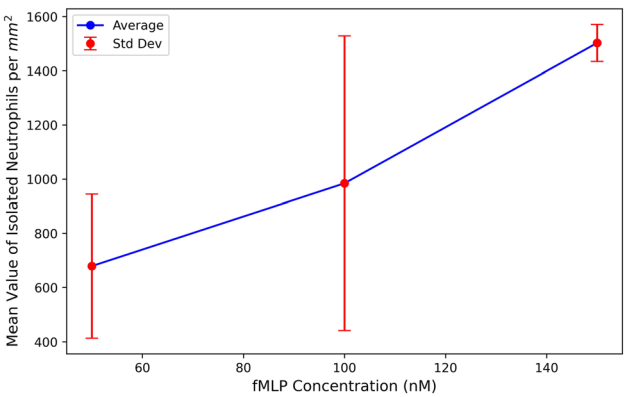

Fig. 4 Effect of fMLP concentration on neutrophil migration. Neutrophils were magnetically isolated from whole blood, adjusted to 2.2 × 10^6 cells per mL, and exposed to increasing concentrations of fMLP (50, 100, and 150 nM). The numbers of neutrophils that migrated into the transmigration chamber were counted. Error bars represent the standard deviation for three replicates (n = 3). The highest migration was observed at 150 nM fMLP.

3.3 Blood dilution optimization

We explored the impact of using whole blood and diluted blood samples (with DPBS + 1 mM EDTA at dilution factors 1 : 1 and 1 : 2) on the number of migrated neutrophils in the bottom chamber (Fig. 5). These experiments examined if decreased sample viscosity or addition of anti-coagulant agents (EDTA) improved the migration of neutrophils.

The results (Fig. 5) indicated that whole blood yielded the highest median number of isolated neutrophils at 125 neutrophils per mm^2 but displayed the widest interquartile range (IQR) compared with diluted blood samples. For 1 : 1 diluted blood, the median number of isolated neutrophils was three times lower than in whole blood at 44 neutrophils per mm^2, yet its IQR was narrower, showing reduced variability in data set. In the case of 1 : 2 dilution, 50 neutrophils per mm^2 was the median count of neutrophils with the least variability among all conditions. These findings indicate that the dilution of blood decreases the number of neutrophils isolated at the bottom chamber. While decreasing the red blood cell density might decrease physical obstructions, diluting also removes important plasma factors, platelets, and soluble signals that promote neutrophil activation and chemotaxis. Our data indicated that the entire blood environment was required for optimal neutrophil transmigration in our platform. This is consistent with previous reports that neutrophil motility is not only affected by mechanical interactions, but also biochemical effects of plasma factors and cell-to-cell interplay.[10]

3.4 Investigating higher fMLP concentration with blood

To increase neutrophil migration to the bottom chamber, we examined the effect of higher fMLP concentrations 150 nM, 300 nM, and 1 μM on the number and viability of neutrophils isolated from whole blood (Fig. 6). At 150 nM, the average number of isolated neutrophils was ~70, while at 300 nM, a slight increase in the mean number of neutrophils was seen at ~72. However, at 1 μM, the number of isolated neutrophils fell to ~27. There were no dead cells across all concentrations, suggesting that larger fMLP dosages do not adversely affect cell viability during the two hours. Since higher fMLP concentrations do not significantly enrich neutrophils, and 150 nM provided consistent results, we chose to proceed with 150 nM for subsequent experiments.

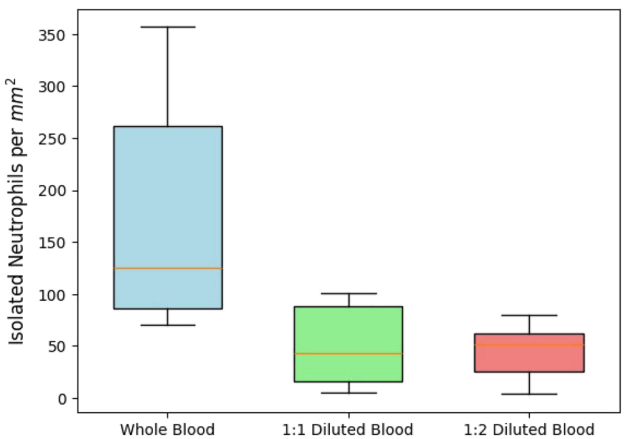

Fig. 5 Effect of blood dilution on the number of migrated neutrophils in the transmigration chamber. Whole blood, 1 : 1 and 1 : 2 diluted blood samples were applied into the blood chamber. Data is shown for five independent repetitions (n = 5), showing the number of isolated neutrophils per mm^2. Whole blood exhibited the highest median and Q1 values, indicating greater neutrophil migration compared to diluted conditions.

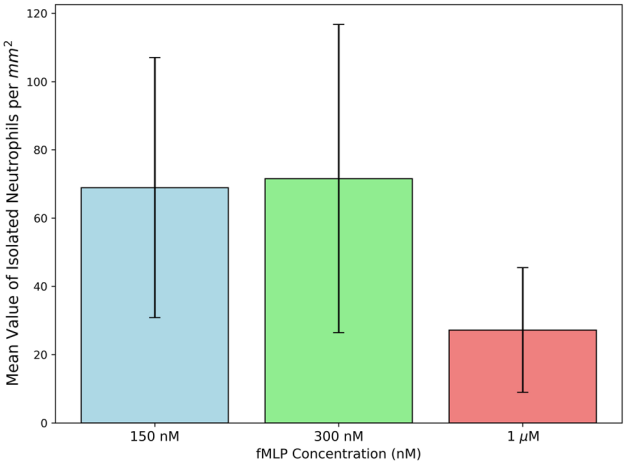

Fig. 6 Effect of higher fMLP concentrations on the number of migrated neutrophils. Whole blood was placed in the top chamber and neutrophil migration was assayed for three different concentrations of fMLP (150 nM, 300 nM, and 1 μM) in triplicate measurements. No significant variation in the migration of neutrophils were observed between 150 nM and 300 nM of fMLP, whereas 1 μM yielded the lowest average.

3.5 Membrane pore size effect

We evaluated the influence of membrane pore size on cell isolation to assess if larger pores facilitated the migration into the bottom chamber and increased the number of isolated neutrophils. A 10 μM pore size membrane was initially used and compared to a 20 μM pore size membrane. For the 10 μM pore size, the mean number of isolated neutrophils was 55, whereas for the 20 μM pore size, the mean number was 80 (see Fig. S3). Although the pore size and number of isolated neutrophils increased, a p-value of 0.2480 indicates that there is no statistically significant improvement in the number of neutrophils isolated. These results, therefore, indicate that increasing the pore size to 20 μM did not facilitate neutrophil isolation.

3.6 Neutrophil isolation under optimized conditions for different healthy samples (donor)

The average number of migrated neutrophils from six healthy samples (donor) was quantified under optimized conditions: 2 mg mL^{-1} ECM collagen concentration, 150 nM fMLP, 10 μM membrane pore size, and whole blood at the top

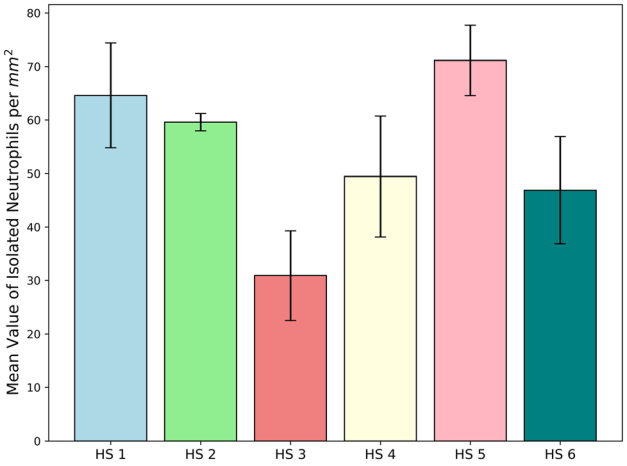

Fig. 7 Mean number of migrated neutrophils across six different blood samples. The experiments were conducted using 2 mg mL^{-1} collagen concentration, 150 nM fMLP, and whole blood applied to the top chamber. The range of number of neutrophils isolated per mm^2 in the transmigrated chamber for these 6 healthy samples (HS) is between 31–71 neutrophils per mm^2.

chamber (Fig. 7). Each whole blood sample was analyzed on the hematology analyzer to attain RBCs, WBCs, neutrophils, and platelet counts prior to every experiment.

The mean number of neutrophils isolated per mm^2 in the bottom chamber for each healthy sample (donor) varied, ranging from the highest count of 71 neutrophils per mm^2 for healthy sample (donor) 5 to a low of 31 neutrophils per mm^2 for healthy sample (donor) 3. It has been shown that various blood components work together to assure an effective immune response. RBCs indirectly regulate neutrophil migration by influencing chemotactic gradients.[26] Platelets are significant mediators of the inflammatory response by actively promoting neutrophil migration towards sites of infection.[27] Other white blood cells assist neutrophil migration during inflammation by sending signals that will attract, guide, or limit their movement. Thus, differences in blood composition between healthy samples (donor), may reflect in neutrophil behavior, hence possibly explaining the inter-healthy sample (donor) variations in respective isolation outcomes.

3.7 Regression analysis

To understand if differences in donor blood cell components influence the number of isolated neutrophils, we examined several correlation models. In these analyses, we assumed the number of isolated neutrophils in the bottom chamber as our dependent variable and the blood cell counts—RBC, WBC, total neutrophils, and platelets—measured by a hematology analyzer prior to the experiment as our independent variables.

For the six data points, the Pearson and Spearman correlation coefficients (ρ) only indicated a strong relationship between isolated neutrophils and the RBC count. For this relationship, the Pearson coefficient was $\rho = 0.73$ with a p-value of 0.09, while the Spearman coefficient was $\rho = 0.71$ with a p-value of 0.11 Although the correlations appear strong, the high p-values (>0.05) indicate the relationship may be due to random chance. For WBC, platelets, and blood neutrophils, correlation coefficients were <0.5 with p-values > 0.1. Therefore, we cannot claim, from this data, that there is a statistically significant linear relationship (in the case of the Pearson correlation) or monotonic relationship (in the case of Spearman correlation) between isolated neutrophils and blood cell counts.

Linear regression analysis showed the relationship between the isolated neutrophils in the bottom chamber and RBC count had the highest R^2 value, of 0.54. For the other blood components, such as WBC, platelets, and total neutrophils, R^2 values were below 0.5. These low R^2 values reveal that linear regression does not fully model the complexity of the number of migrated neutrophils with respect to blood component counts. Thus, there are possible influences from the combination of the variables or non-linear dynamics at play.

For this, non-linear exponential growth/decay, logistic function and polynomial models were applied. The exponential model generated a poor fit, as evidenced by a R^2 value of 0. The logistic regression model produced R^2 values from 0.60 to 0.65, with the highest value observed for the relationship between isolated neutrophils and platelets. This relationship had a negative growth rate indicating that as the platelets increase, the isolated neutrophils variable decrease, but the relationship was subtle because the magnitude of slope is small.

Polynomial regression showed insignificant R^2 values for isolated neutrophils and RBC, WBC, and blood neutrophils at 0.54, 0.55, and 0.42, respectively. The highest fit ($R^2 = 0.88$) was observed for the relationship between isolated neutrophils in the bottom chamber and platelets. The polynomial coefficients (see Fig. S4) for this relationship suggests that isolated neutrophils initially increase with platelets but eventually reach a peak and start to decrease.

Based on our analysis, among all blood components, RBCs may have a linear relationship with isolated neutrophils. This is supported by moderate Spearman and Pearson coefficients with high p-values. RBCs counts also had the highest R^2 in the linear regression model. However, high p-values and insufficient R^2 values do not confirm this relationship. Further investigation with a larger data set is needed for a comprehensive understanding of the relationship between RBCs and transmigrated neutrophils. Although the sample size is limited, polynomial regression analysis did show platelets have a strong non-linear effect on neutrophil isolation where neutrophils and platelets follow a saturation model. Beyond a certain threshold, increases in platelets do not have proportional returns in neutrophil isolation. These results provide an initial framework for further investigations about the blood components that may affect neutrophil isolation and the biological mechanisms involved.

4 Discussion

We developed and characterized an *in vitro* inflammation model that allowed the study of neutrophil transmigration from whole blood. For our model, we optimized an ECM composed of collagen and Geltrex that replicates the blood–ECM interface. Similarly, to *in vivo* conditions, the ECM only allows neutrophils to transverse during an inflammation chemotactic-induced event, while inhibiting the migration of other blood cells and components. Using inexpensive rapid prototyping techniques, we fabricated a stacked well system that embedded the ECM between a top and bottom chamber. Blood filled the top chamber and, in the bottom well, fMLP was used as a chemoattractant to mimic inflammation, attracting neutrophils from whole blood into the matrix and then into the bottom well. In the bottom well, enriched migrated neutrophils were captured and optically characterized.

Unlike other inflammation models that rely on 2D surfaces, require pre-processed isolated neutrophils, or microfabricated RBC filters, our model implements a tunable 3D collagen–Geltrex ECM. By considering the effect of collagen concentration, we modified our matrix structure. We observed that high collagen concentrations (2 mg mL^{-1}) hindered neutrophils as well as other blood cells from freely trespassing the ECM. According to previous studies, concentrations of collagen type I at 2 mg mL^{-1}, generate pore sizes between 1–3 μM.[28] These pore sizes are far below blood cell diameters which range between 6–20 μM, and neutrophil diameters which fall between 13–18 μM. Thus, it is only after the addition of fMLP that a gradient is established across the ECM causing neutrophils in whole blood to interact with chemoattractant molecules and undergo cytoskeleton and morphology changes. Neutrophils flatten, polarize and squeeze through the matrix pores towards the gradient source in the bottom chamber.[29,30]

In the bottom well, purified neutrophils were microscopically visualized and confirmed by their unique multi-lobed nuclei. We never observed other cell types in the bottom chamber during the two-hour assay period and fMLP concentrations tested. fMLP is a familiar chemoattractant that primarily recruits neutrophils due to their higher levels of formyl peptide receptors (FPR)[31] specifically, FPR1, compared to other cell types. Though other studies have shown that fMLP chemoattracts monocytes, basophils, and eosinophils, these cells are far less responsive to fMLP compared to neutrophils and often require higher concentrations or a 6 h delay to respond.[32]

Similar to other studies, in our inflammation model, we did observe changes in migrated population for different fMLP concentrations tested. We found that increasing concentrations of fMLP between 50–150 nM expanded the migrated neutrophil population in the bottom well, but concentrations of 1 μM depleted neutrophil migrated population by 60%. Previously, it was reported that fMLP concentrations of 50–150 nM showed steeper gradients for higher concentrations, consequently leading to faster diffusion rates and maximizing the recruitment of neutrophils. In this concentration range, neutrophils showed optimal chemotactic response with strong and directed movement toward the chemoattractant source.[33] In contrast, higher concentrations of 1 μM fMLP result in receptor desensitization and, as a consequence, decrease in chemotactic polarization efficiency, causing random cell movement.[34] This suggests that our platform generates chemical gradients across the ECM like those generated in more traditional microfluidic systems that involve tedious pumping systems, or sophisticated microfluidic channel design and fabrication.

While other inflammation models require dilutants for the analysis of whole blood samples, our model isolates neutrophils from unprocessed (undiluted) whole blood as well as diluted blood samples. In our model, we observed that whole blood presented the highest number of isolated neutrophils compared to 1 : 1 or 1 : 2 diluted blood samples. Because our sample is not confined to a small channel cavity, activated and deformable neutrophils can move with more ease around RBCs and other blood cells towards the gradient source. While diluting a sample can increase the distance between cells and facilitate cell movement, in our device, it decreased the number of available neutrophils to migrate.

Working with whole blood samples, however, we did see large differences in neutrophil isolation between healthy samples (donor). Because blood components actively participate in neutrophil transmigration and are not the same in each healthy sample (donor), they may contribute to the variation observed. RBCs may restructure the ECM pore sizes because of their mass, acting as a physical barrier for migration. The presence of RBCs may also influence chemotactic gradients *via* chemokine binding or setting oxygen levels by releasing oxygen into the surrounding tissue which affect neutrophil metabolism, activation, and impacting movement indirectly.[26,27] Similarly, platelets increase neutrophil surface adhesion *via* the interaction between P-selectin and PSGL-1 and release chemotactic factors to guide the migration.[35,36] In addition, other white blood cells, such as monocytes, release cytokines that modulate neutrophil activation and recruitment. The interplay between all these components will affect neutrophil behavior. Thus, regression analysis was used to investigate if the variability in migrated neutrophils among healthy samples (donor) were influenced by blood composition-number of neutrophils, RBCs, WBCs, and platelets. Based on our regression analysis, we found the higher blood neutrophil counts do not result in higher isolated neutrophils. It is possible that other factors such as the activation states of neutrophils drive their transmigration behavior. Also, we found that there is no linear pattern between isolated neutrophils in the bottom chamber and blood components. Instead, we did observe that in comparing all the blood components, platelets satisfied a second-degree polynomial regression model with R^2 = 0.88.

This indicates that at lower platelets levels, isolated neutrophils increase, but at higher platelets levels, neutrophil isolation can decrease, suggesting a saturation or plateau effect. This model points to nonlinear dynamics between isolated neutrophils and platelets. Platelets generally support neutrophil migration *via* adhesion support and inflammatory signaling; however, under extreme activation or aggregation many bioactive molecules, such as thrombospondin-1 and transforming growth factor-beta (TGF-β) are released, which may inhibit the motility of neutrophils. Also, at high numbers of platelets, platelet aggregates increase. It is possible that neutrophils tend to get stuck and attached to platelet aggregates rather than migrating effectively through the ECM. Our initial results corroborate this understanding of platelet behavior.

Though, we only presented the quantification and viability of transmigrated neutrophils during fMLP inflammation challenges, our microfluidic platform can have broader applications including the examination of inflammation resolution mechanisms as well as neutrophil immune response to different stimuli and therapeutics. In the inflammation process, after neutrophils transmigrate the ECM and tissue, they address threats using various defense mechanisms. Then, they undergo apoptosis as an initial step in resolving inflammation.[37] Using our platform, post-transmigration neutrophil phenotypes can be examined using fluorescent labels and microscopy to determine how resolution evolves between diseased and non-diseased populations. Additionally, our platform can explore neutrophil immune response to different pathogen sources by replacing fMLP with other chemoattractant or pathogen agents in the transmigration wells. Our platform can also be used to examine different drugs that modify neutrophil transmigration and post-transmigration behavior. Due to the multi-well design, which can be expanded to a larger array if required, we can run multiple condition experiments on the same device. As a result, our well based chip design can simplify the experimentation involved in inflammation studies while still enhancing the physiological relevance due to the incorporation of the ECM and utilization of whole blood. It eliminates the need for traditional, laborious and potentially harmful neutrophil isolation methods. Thereby, our inflammation platform can provide a useful tool for the investigation of different inflammation pathologies and treatments.

Conclusions

We successfully developed an *in vitro* inflammation model that replicates an inflammation event and directly isolates highly pure neutrophils from unprocessed whole blood. Like in the body, in this model, neutrophils migrate from whole blood through a 3D ECM toward a chemoattractant source. This approach not only accomplished passive isolation but also enabled *in vivo*-like 3D transmigration of neutrophils. Our findings demonstrated that the ECM composition, chemoattractant concentration, and blood conditions influence the size of transmigrated neutrophil population. In addition, preliminary regression modeling indicated that platelet quantity may impact the number of transmigrated neutrophils, satisfying a non-linear saturation model. Such a platform can be useful in the study of immune cell behavior in inflammatory conditions, inflammation-related diseases, and anti-inflammatory drugs.

Ethical statement

All human blood samples used in this study were obtained from the Stanford Blood Center as fully de-identified specimens from healthy donors. The investigators had no access to identifying information and no interaction with the donors. Under the U.S. Department of Health and Human Services regulations (45 CFR 46), the use of these de-identified samples does not constitute human-subjects research. Accordingly, this study was considered exempt from Institutional Review Board (IRB) oversight and approval. All donors provided informed consent to the Stanford Blood Center for the collection and use of their blood for research purposes, in accordance with institutional policies and applicable regulations.

Resource for this information can be found here: https://grants.nih.gov/grants/policy/hs/private-information-biospecimens-flowchart.pdf.

Conflicts of interest

There are no conflicts to declare.

Data availability

All data supporting the findings of this study are available from the corresponding author upon request.

Supplementary information (SI) is available. See DOI: https://doi.org/10.1039/d5lc00554j.

Acknowledgements

We thank the Open Medicine Foundation for funding this project. We also thank Whitney Dafoe for raising funds for this research.

Notes and references

1 M. T. Quinn, F. R. DeLeo and G. M. Bokoch, *Neutrophil methods and protocols*, Springer, 2007, vol. 412.
2 J. Degel and M. Shokrani, *American Society for Clinical Laboratory Science*, 2010, **23**, 94–98.
3 K. Hoebe, E. Janssen and B. Beutler, *Nat. Immunol.*, 2004, **5**, 971–974.
4 F. Wang, *Cold Spring Harbor Perspect. Biol.*, 2009, **1**, a002980.
5 K. V. Sawant, K. M. Sepuru, E. Lowry, B. Penaranda, C. W. Frevert, R. P. Garofalo and K. Rajarathnam, *J. Leukocyte Biol.*, 2021, **109**, 777–791.

6 D. J. Brat, A. C. Bellail and E. G. Van Meir, *Neuro-Oncology*, 2005, **7**, 122–133.
7 H. L. Wright, R. J. Moots, R. C. Bucknall and S. W. Edwards, *Rheumatology*, 2010, **49**, 1618–1631.
8 A. Herrero-Cervera, O. Soehnlein and E. Kenne, *Cell. Mol. Immunol.*, 2022, **19**, 177–191.
9 J. G. Filep, *Front. Immunol.*, 2022, **13**, 866747.
10 S. De Oliveira, E. E. Rosowski and A. Huttenlocher, *Nat. Rev. Immunol.*, 2016, **16**, 378–391.
11 B. V. Ineichen, E. Furrer, S. L. Grüninger, W. E. Zürrer and M. R. Macleod, *PLoS Biol.*, 2024, **22**, e3002667.
12 R. B. Riddle, K. Jennbacken, K. M. Hansson and M. T. Harper, *Sci. Rep.*, 2022, **12**, 6855.
13 P. H. McMinn, L. E. Hind, A. Huttenlocher and D. J. Beebe, *Lab Chip*, 2019, **19**, 3697–3705.
14 H. W. Hou, A. A. S. Bhagat, W. C. Lee, S. Huang, J. Han and C. T. Lim, *Micromachines*, 2011, **2**, 319–343.
15 C. J. O. Bacal, J. W. Maina, H. H. Nandurkar, M. Khaleel, R. Guijt, Y. Chang, K. M. Dwyer and L. F. Dumée, *Mater. Adv.*, 2021, **2**, 7210–7236.
16 S. Fukuda and G. W. Schmid-Schönbein, *J. Leukocyte Biol.*, 2002, **72**, 133–139.
17 J. Lundahl, G. Hallden, M. Hallgren, C. Sköld and J. Hed, *J. Immunol. Methods*, 1995, **180**, 93–100.
18 C. Van Oss, P. Bronson, E. Dinolfo and K. Chadha, *Immunol. Commun.*, 1981, **10**, 549–555.
19 K. Lang, Mechanisms of suicidal erythrocyte death, *Cell. Physiol. Biochem.*, 2005, **15**, 195–202.
20 M. Blanter, S. Cambier, M. De Bondt, L. Vanbrabant, N. Pörtner, S. Abouelasrar Salama, M. Metzemaekers, P. E. Marques, S. Struyf and P. Proost, *et al.*, *Front. Immunol.*, 2022, **13**, 820058.
21 K. T. Kotz, W. Xiao, C. Miller-Graziano, W.-J. Qian, A. Russom, E. A. Warner, L. L. Moldawer, A. De, P. E. Bankey and B. O. Petritis, *et al.*, *Nat. Med.*, 2010, **16**, 1042–1047.
22 N. Agrawal, M. Toner and D. Irimia, *Lab Chip*, 2008, **8**, 2054–2061.
23 B. Hamza and D. Irimia, *Lab Chip*, 2015, **15**, 2625–2633.
24 C. N. Jones, A. N. Hoang, L. Dimisko, B. Hamza, J. Martel and D. Irimia, *J. Visualized Exp.*, 2014, 51215.
25 J. François, A. Kandasamy, Y.-T. Yeh, A. Schwartz, C. Ayala, R. Meili, S. Chien, J. C. Lasheras and J. C. Del Álamo, *Sci. Adv.*, 2021, **7**, eabf3882.
26 L. Ottonello, M. Ghio, P. Contini, M. Bertolotto, G. Bianchi, F. Montecucco, M. Colonna, C. Mazzei, F. Dallegri and F. Indiveri, *Transfusion*, 2007, **47**, 1395–1404.
27 S. Pitchford, D. Pan and H. C. Welch, *Curr. Opin. Hematol.*, 2017, **24**, 23–31.
28 A. D. Doyle, *Curr. Protoc. Cell Biol.*, 2016, **72**, 10–20.
29 S. Denk, R. P. Taylor, R. Wiegner, E. M. Cook, M. A. Lindorfer, K. Pfeiffer, S. Paschke, T. Eiseler, M. Weiss and E. Barth, *et al.*, *Scand. J. Immunol.*, 2017, **86**, 143–155.
30 S. Dewitt, R. J. Francis and M. B. Hallett, *J. Cell Sci.*, 2013, **126**, 4627–4635.
31 Y. Le, P. M. Murphy and J. M. Wang, *Trends Immunol.*, 2002, **23**, 541–548.
32 G. Monneret, M. Gutowski and J. Bienvenu, *Clin. Exp. Immunol.*, 1999, **115**, 393–396.
33 A. Chandrasekaran, F. Ellett, J. Jorgensen and D. Irimia, *Microsyst. Nanoeng.*, 2017, **3**, 1–8.
34 O. Iizawa, H. Akamatsu and Y. Niwa, *Neurosignals*, 2004, **4**, 14–18.
35 T. Xu, L. Zhang, Z. H. Geng, H.-B. Wang, J.-T. Wang, M. Chen and J.-G. Geng, *Cell Adhes. Migr.*, 2007, **1**, 115–123.
36 F. W. Lam, A. R. Burns, C. W. Smith and R. E. Rumbaut, *Am. J. Physiol.*, 2011, **300**, H468–H475.
37 E. Kolaczkowska and P. Kubes, *Nat. Rev. Immunol.*, 2013, **13**, 159–175.